J Supercond Nov Magn (2013) 26:1099–1103
DOI 10.1007/s10948-012-1918-1

ORIGINAL PAPER

Effect of Al Substitution on Structural and Electrical Properties of $Bi_{1.6}Pb_{0.4}Sr_2CaCu_{2-x}M_xO_{8+\delta}$ Superconducting Ceramics

F. Bouaïcha · M.-F. Mosbah · M. Hamel · F. Benmaamar · A. Amira · T. Guerfi · A. Haouam · L. Ozyuzer

Received: 7 November 2012 / Accepted: 30 November 2012 / Published online: 28 December 2012

Abstract In this work we study the effect on structural and electrical properties of superconducting compound $Bi_{1.6}Pb_{0.4}Sr_2CaCu_{2-y}M_yO_{8+\delta}$ were M = Al (with y = 0–0.6). The samples were prepared by the solid-state reaction method. The samples have been characterized by X-ray diffraction (XRD), scanning electron microscopy (SEM), direct current (DC) resistivity versus temperature $\rho(T)$ and alternative current (AC) susceptibility measurements. Structural analysis shows that the crystalline lattice structure of the prepared sample belongs, mainly, to the superconductive tetragonal phase Bi(Pb)2212. The SEM micrographs show that in the undoped sample the grain size has a random distribution with few grains greater than 5 μm. The grains are very dense and well connected. A quite different microstructure is obtained for the doped samples of which grains are more connected with a flat characteristic shape of Bi(Pb)2212 superconductors. All samples exhibit a superconducting character and T_c and the superconducting volume fraction decrease with increasing rate of aluminum.

Keywords Superconductivity · SHTC · Bi–Pb–Sr–Ca–Cu–O system · Substitution · Doping · Resistivity · Normal state

F. Bouaïcha (✉)
Materials Sciences Department, Larbi Ben M`hidi University, B.P. 358, 04000 Oum El Bouaghi, Algeria
e-mail: bou_faiza@yahoo.fr

F. Bouaïcha · M.-F. Mosbah · M. Hamel · F. Benmaamar · T. Guerfi
Material Science and Applications Research Unit, Physics Department, Mentouri University, Route de Ain-el-Bey, 25017 Constantine, Algeria

A. Amira
Non-Destructive Testing Laboratory, Faculty of Sciences and Technology, University of Jijel, B.P. 98, Ouled Aissa, Jijel 18000, Algeria

T. Guerfi
Department of Physics, Faculty of Sciences, M'hamed Bougara University, Boumerdes, 35000, Algeria

A. Haouam
Electronic Department, Faculty of Engineering Sciences, Mentouri University, Route de Ain-el-Bey, 25017 Constantine, Algeria

L. Ozyuzer
Department of Physics, Izmir Institute of Technology, 35430 Izmir, Turkey

1 Introduction

Since the discovery of superconductivity many researchers have devoted their time and enthusiasm to understand this incredible drop in resistivity. Among them we cite Meissner, London brothers, Ginzburg, Landau, Bardeen, Cooper and Schrieffer. Unfortunately, the first materials tested had very low critical temperatures, making applications difficult to several decades. Superconductivity became gradually forget to the general public so that its use was limited to laboratories. The discovery by Bednorz and Muller in 1986 of superconductivity at 30 K in oxide material based on barium, lanthanum and copper LaBaCuO revived the interest of the scientific community to the phenomenon [1]. In 1987 Wu et al. [2] synthesized $YBa_2Cu_3O_{7-\delta}$ an oxide superconducting at 92 K. Subsequently Maeda et al. [3] discovered superconductivity in the BSCCO system. The family of compounds $Bi_2Sr_2Ca_{n-1}Cu_nO_{2n+4}$ consists essentially of three superconducting phases: Bi2201, Bi2212 and Bi2223 [4, 5] with $n = 1, 2, 3$, respectively, corresponding to number of CuO_2 planes in their structure. Among these phases, the first phase

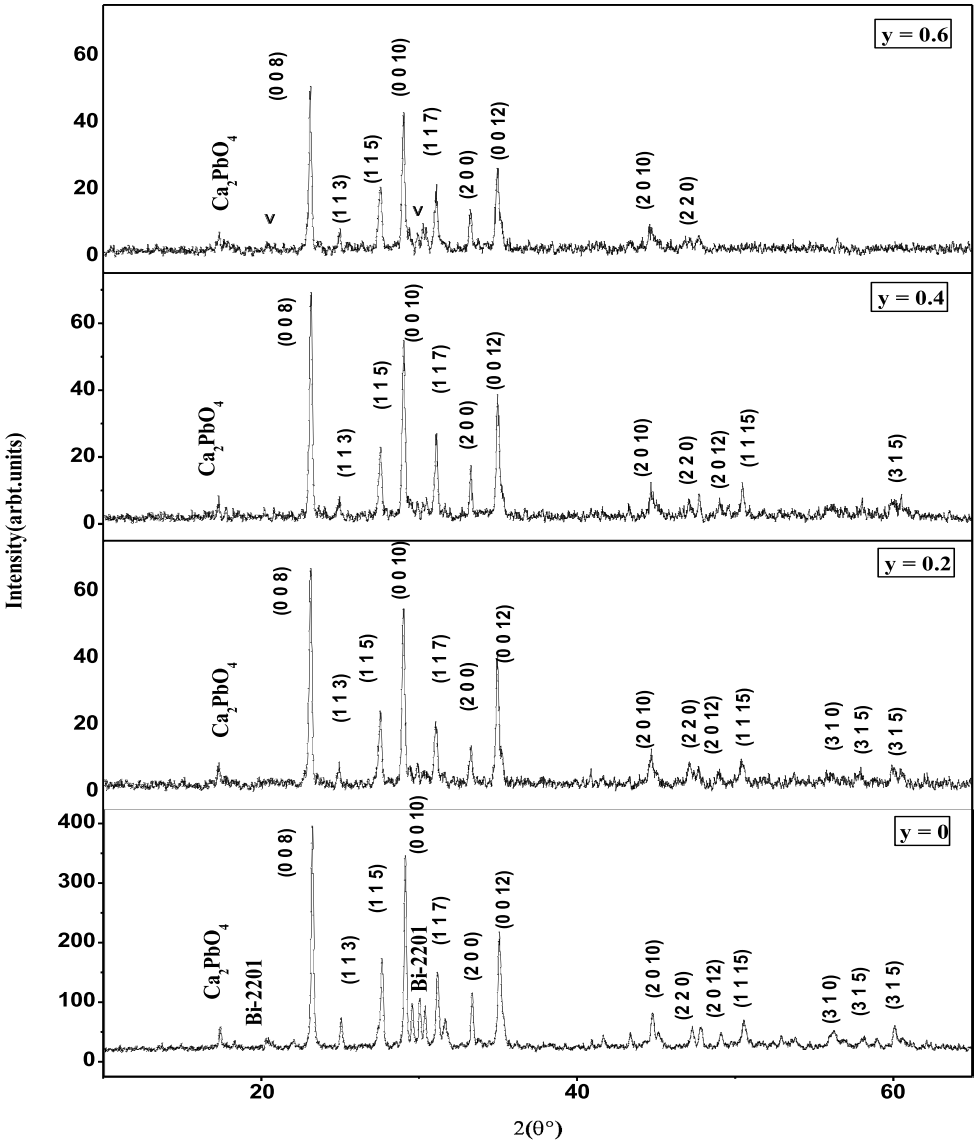

Fig. 1 X-ray diffraction patterns of the $Bi_{1.6}Pb_{0.4}Sr_2CaCu_{2-y}Al_yO_{8+\delta}$ samples

(Bi2212) is discovered in 1988 [3]. The partial substitution of Bi by Pb enhances the formation and increases the volume fraction of BSCCO phases with high critical temperature as indicated by numerous studies [6, 7]. In the Bi2212 phase, the Bi substitution by Pb results in a remarkable improvement of the superconductive properties. Moreover, if oxygen stoichiometry is well controlled, a great improvement of the density of critical current is possible up to 77 K [8–10]. Doping by magnetic and non-magnetic atoms can change the superconducting properties of high critical temperature superconductors. When the Cu sites in the CuO_2 planes are involved the change can reduce dramatically the critical temperature T_c and even kill the superconductivity. These kinds of doping have been made in order to control the charge carrier concentration in these planes and consequently to control the superconducting properties. The results obtained in Bi2212 [11–13] by doping with Fe, Zn, Ni or Co, have shown that the situation is a little more complex. The sample shows, in its normal state, a behavior interpreted by some authors as a pseudo gap and by others as a quantum critical point [14–16].

According to our knowledge in Bi-2212, studies made until now have concerned only free lead samples. Lead is known to improve [17], with a limited concentration, the superconducting properties and may be a way to control the doping by other elements. For that purpose, $Bi_{1.6}Pb_{0.4}Sr_2CaCu_{2-y}Al_yO_{8+d}$ samples, with $y = 0$–0.06, have been prepared using the solid-state reaction technique.

2 Experiments

Samples of $Bi_{1.6}Pb_{0.4}Sr_2CaCu_{2-y}Al_yO_{8+\delta}$, with $0 \leq y \leq 0.6$, were prepared by conventional solid-state reaction

Table 1 Cell parameters $\boldsymbol{a}$ and $\boldsymbol{c}$, residual resistivity r_0, T_c^{onset}, $T_c(0)$ and ΔT of the samples

Rate of Al	$\boldsymbol{a}$ (A°)	$\boldsymbol{c}$ (A°)	ρ_0 (mΩcm)	T_c^{onset} (K)	$T_c(0)$ (K)	ΔT (K)
0	5.398	30.845	10	80.8	48.8	32
0.2	5.228	30.840	1.85	72.3	55.5	16.8
0.4	5.408	30.866	5	71.3*	41	29.7
0.6	5.396	30.845	–	70*	–	

*Deduced from AC susceptibility

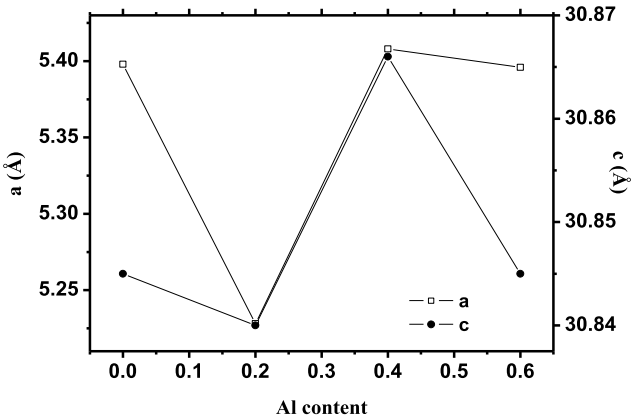

Fig. 2 Variation of $\boldsymbol{a}$- and $\boldsymbol{c}$-axis cell parameter with the rate of Al

method. High grade purity powders of Bi_2O_3, PbO, $SrCO_3$, $CaCO_3$, CuO and Al_2O_3, weighed in stœchiometric ratio, were mixed and ground in an agate mortar, put in a cylindrical crucible and calcined in a two steps procedure: the first at 800 °C for 10 h and the second at 810 °C for 30 h. The prepared powders were successively grinded, pressed in pellet shape under a pressure of 225 MPa and sintered twice at 840 °C during 50 h. The heating rate was 5 °C/min. Structural properties and phase purity were characterized by X-ray powder diffraction (XRD) using CuK_α radiation of copper ($\lambda_{CuK\alpha} = 1.5418$ Å) in a Siemens D8-Advance type diffractometer operating in Bragg-Brentano geometry. Identification of the existing phases was carried out with the help of JCPD-ICDD data file [18]. The lattice parameters of the Bi(Pb)2212 and Bi(Pb,Al)-2212 phases were identified using DicVol software [19]. Microphotographies were taken using Scanning Electron Microscope (SEM). The DC electrical resistivity $\rho(T)$ was measured by a classical four probe technique. AC susceptibility was measured using a homemade probe and an AC field with 50 A/m of amplitude and 820 Hz of frequency.

3 Results and Discussion

3.1 XRD Analysis

The XRD patterns of the obtained Bi(Pb)2212 and aluminum doped samples ($y = 0.2$; 0.4 and 0.6) are shown in Fig. 1, with the Miller indices of the corresponding diffracting planes. The majority of the identified peaks belong to the Bi(Pb)2212 phase, which is accompanied by traces of the parasitic Bi-2201 and Ca_2PbO_4 phases. This last one is identified by a peak for $2\theta = 17.68°$ which intensity is reduced by the introduction of aluminum. Aluminum induces also a reduction of the intensities of the main peaks (0 0 8), (0 0 10) and (0 0 12) of the Bi(Pb)2212 phase. These results show that the Al atoms enter into the lattice. The intensities of the main peaks are relatively higher than those of the other planes suggesting a preferential orientation of the grains in the [0 0 l] direction. Aluminum induces also a displacement of the peaks to the left. The amplitude of the displacement is practically the same for all peaks, about $2\theta = 0.12°$, except for the (0 0 8) peaks which is slightly higher, of the order of $2\theta = 0.14°$.

The cell parameters, obtained with DicVol software, show that the obtained phases are tetragonal. These parameters summarized in Table 1 are in agreement with those reported in the literature [20, 21]. In Table 1 there are also the residual resistivity ρ_0, the T_c^{onset}, the $T_c(0)$ and the ΔT deduced from resistivity and AC susceptibility curves. As shown by Fig. 2, the cell parameters $\boldsymbol{a}$ and $\boldsymbol{c}$ are firstly reduced for $y = 0.2$, and then go, for $y = 0.4$, through a maximum higher than the undoped sample one. For $y = 0.6$, the cell parameters are identical to the undoped sample one. The ionic radius of Al^{+3} (0.48 Å) is lower than that of Cu^{+2} (0.65 Å) [22]. The contraction of the $\boldsymbol{c}$-axis cell parameter is then naturally expected. On the other hand, Al^{+3} ion with outer electronic shell $2s^2 2p^6$ configuration is without magnetic spin moment (spinless). The substitution of Cu^{+2} by Al^{+3} involves two types of modification: increase of charge carriers and a local depletion of magnetic moment. The increase of the density of charge carriers in the CuO_2 planes may also cause a contraction of the $\boldsymbol{c}$-axis. This effect, accompanied by a contraction of the $\boldsymbol{a}$ axis, is observed only for $y = 0.2$. The substitution of a Cu^{+2} ion, which is in $3d^9$ configuration, by an Al^{+3} ion, in $2p^6$ configuration, changes the local Jahn Teller distortion expected for the octahedrons formed by Cu surrounded by oxygen atoms in the CuO_2 planes. The excess of charge carriers generated by the high rate of Al doping in the Cu site may then result in the observed increase of the $\boldsymbol{c}$-axis cell parameter.

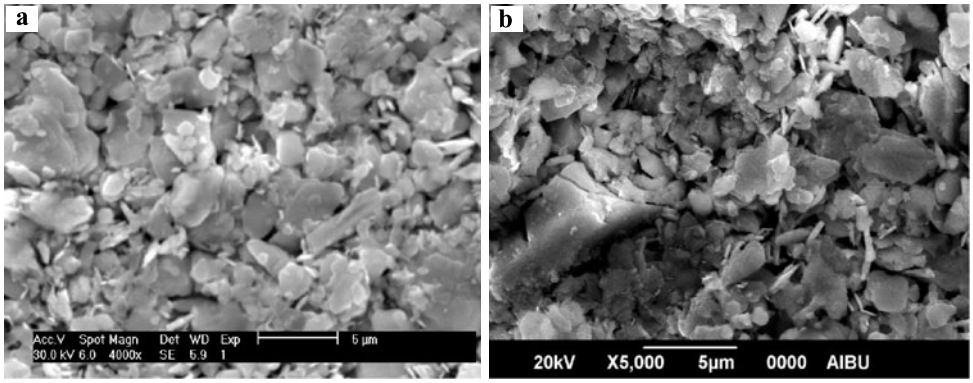

Fig. 3 SEM micrographs of undoped (**a**) and doped ($y = 0.4$) (**b**) samples

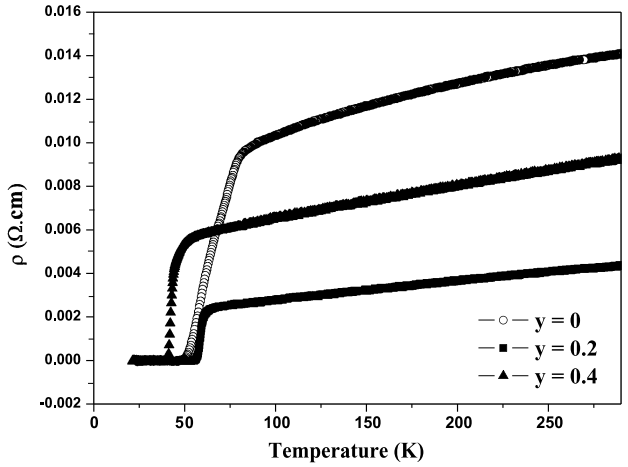

Fig. 4 Resistivity versus time measurements $\rho(T)$ of the samples where: ○ undoped; ■ $y = 0.2$; ▲ $y = 0.4$

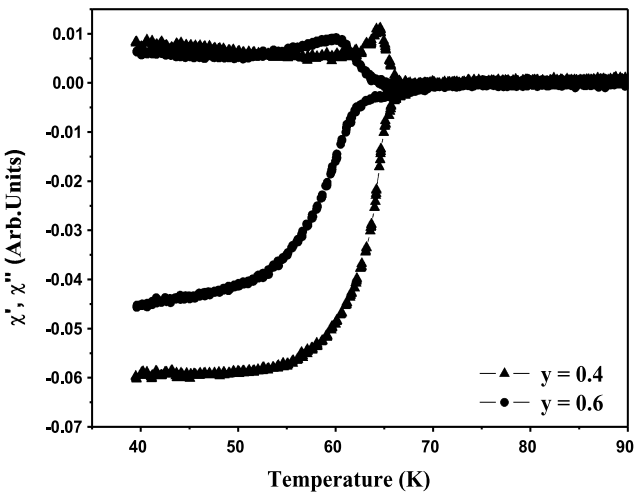

Fig. 5 AC susceptibility of samples with: ▲ $y = 0.4$; ◆ $y = 0.6$

3.2 SEM Analysis

Figure 3 shows SEM photographs of two samples. The undoped sample (Fig. 3a) shows the layered structure which characterizes the growth of Bi(Pb)2212 grains. Small white nodules, due to some precipitate of the starting powders, can be noticed. The grains appear rather dense and well connected. The morphology of the grains of the doped samples is different (Fig. 3b) with the same flattened shape and distribution of size and orientation seeming more random. The porosity is greater when aluminum is present. Big white nodules may be observed.

3.3 Resistivity and AC Susceptibility Measurements

The variation of the resistivity with temperature is shown in Fig. 4. The part of the curves corresponding to the normal state shows that the density of charge carriers varies with y. This density is inversely proportional to the residual resistivity ρ_0 deduced from the extrapolation of the normal part of $\rho(T)$ near 300 K to 0 K and reported in Table 1. ρ_0 has the lowest value for $y = 0.02$.

The corresponding sample has also the lowest width of transition ΔT which is reported in Table 1 and represents the difference between T_c^{onset} and $T_c(0)$. The sample with $y = 0.4$ has a same ΔT than the undoped one. The introduction of aluminum results in a decrease in T_c^{onset} of about 8.5 K for $y = 0.2$ until 10 K for $y = 0.6$. On the contrary $T_c(0)$, which is for the undoped sample 48.8 K, increases for $y = 0.2$ to 55.5 K then decreases to 41 K for $y = 0.4$. The decrease of T_c^{onset} is expected because Al substitutes on the Cu site and introduces some perturbations in the CuO_2 planes. The lowest value of ρ_0 and ΔT for $y = 0.2$ indicates, however, that improvement may be obtained at low rate of doping.

The real $\chi'(T)$ and imaginary $\chi''(T)$ part of the AC susceptibility are shown in Fig. 5 for $y = 0.4$ and $y = 0.6$. These curves indicates that the apparent superconducting volume fraction, proportional to the value at lowest temperature of χ', decreases with the rate y of aluminum. The increase of the rate of aluminum causes also an increase of the transition width and a displacement toward lower temperature of the maximum of $\chi''(T)$, indicating an increase of defects in grains and degradation of grain boundaries.

4 Conclusions

In summary, doping by Al in Bi(Pb)2212 decreases the T_c^{onset} but for low rate ($y = 0.2$) higher conductivity in the normal state is obtained and the transition width is lowered and at the same time the $T_c(0)$ has the highest value compared with the undoped sample. Increasing the rate of aluminum decreases the apparent superconducting volume fraction and degrades the quality of grains and grain boundaries.

References

1. Bednorz, G., Müller, K.A.: Z. Phys. B, Condens. Matter **64**, 189 (1986)
2. Wu, M.K., Ashburn, J.R., Torng, C.J., Hor, P.H., Meng, R.L., Gao, L., Huang, Z.J., Wang, Y.Q., Chu, C.W.: Phys. Rev. Lett. **58**, 908 (1987)
3. Maeda, H., Tanaka, Y., Fukutomi, M., Asono, T.: Jpn. J. Appl. Phys. **27**, L209–210 (1988)
4. Chu, S., McHenry, M.E.: J. Mater. Res. **13**, 589 (1998)
5. Lee, T.J., Huang, C.F., Teo, C.C., Khor T, S., Ku, H.C., Yeh, K.W., Huang, Y., Hung, H.H., Sakabe, K., Sakabe, N.: Chin. J. Phys. **38**, 243 (2000)
6. Meretliv, Sh., Sadykov, K.B., Beerkeliev, A.: Turk. J. Phys. **24**, 39 (2000)
7. Hooker, M.W., Martin, L.: NASA Contractor Report 4761, Engineering & Sciences Company, Hampton, Virginia (1996)
8. Chong, I., Hiroi, Z., Izumi, M., Shimoyama, J., Nakayama, Y., Kishio, K., Terashima, T., Bando, Y., Takano, M.: Science **276**, 770 (1997)
9. Shimoyama, J., Nakayama, Y., Kitazawa, K., Kishio, K., Hiroi, Z., Chong, I., Takano, M.: Physica C **281**, 69 (1997)
10. Shimoyama, J., Murakami, K., Shimizu, K., Nakayama, Y., Kishio, K.: Physica C **357–360**, 1091 (2001)
11. Kuo, Y.K., Schneider, C.W., Skove, M.J., Nevitt, M.V., Tessema, G.X., McGee, J.J.: Phys. Rev. B **56**, 6201 (1997)
12. Zhao, X.R., Kitazawa, K., Hasegawa, T.: Physica C **370**, 44 (2002)
13. Uprety, K.K., Horvat, J., Wang, X.L., Ionescu, M., Liu, H.K., Dou, S.X., Brandt, E.H.: Phys. Rev. B **65**, 224501 (2002)
14. Yurgens, A., Winkler, D., Claeson, T., Hwang, S.J., Choy, J.H.: Physica C **362**, 286 (2001)
15. Ekino, T., Hashimoto, S., Fujii, H.: Physica C **357–360**, 130 (2001)
16. Miyakawa, N., Zasadzinski, J.F., Oonuki, S., Asano, M., Henmi, D., Kaneko, T., Ozyuzer, L., Gray, K.E.: Physica C **364–365**, 475 (2001)
17. Wang, X.L., Liu, H.K., Dou, S.X.: Physica C **364–365**, 622 (2001)
18. PDF-2 Database 47 6A Jun 97 JCPD-ICDD USA (1997)
19. Boultif, A., Louër, D.: J. Appl. Crystallogr. **37**, 724 (1991)
20. Altin, S., Aksan, M.A., Balci, Y., Yakinci, M.E.: J. Phys. Conf. Ser. **153**, 012004 (2009)
21. Lovleena, Bidikin, I.K., Kholkin, A.L., Kumar, B.: Physica C **451**, 44 (2007)
22. Shannon, R.D.: Acta Crystallogr. A **32**, 751 (1976)